Atmospheric Environment 229 (2020) 117484

Contents lists available at ScienceDirect

Atmospheric Environment

journal homepage: http://www.elsevier.com/locate/atmosenv

Source apportionment of water-soluble brown carbon in aerosols over the northern South China Sea: Influence from land outflow, SOA formation and marine emission

Xiaofei Geng [a,b], Yangzhi Mo [a], Jun Li [a], Guangcai Zhong [a,**], Jiao Tang [a,b], Hongxing Jiang [a,b], Xiang Ding [a], Riffat Naseem Malik [c], Gan Zhang [a,*]

[a] State Key Laboratory of Organic Geochemistry, Guangzhou Institute of Geochemistry, Chinese Academy of Sciences, Guangzhou, 510640, China
[b] University of Chinese Academy of Sciences, Beijing, 100049, China
[c] Quaid-i-Azam University, 45320, Pakistan

HIGHLIGHTS

- WSOC in a round-year set of samples were characterized for optical properties.
- Elevated land outflow of water-soluble BrC with high MAE_{365} was observed in winter.
- Biomass burning and urban SOA & waste combustion were main sources of Abs_{365}.
- WSOC from biomass burning and urban SOA & waste combustion showed high MAE_{365}.
- Microorganism/plankton primary emission was a major source of Abs_{365} in spring.

ARTICLE INFO

Keywords:
Water-soluble brown carbon
Light absorption properties
Molecular markers
Atmospheric outflow
Source apportionment

ABSTRACT

Water-soluble brown carbon (BrC) plays an important role in climate change by influencing aerosol radiative forcing. There is little information on aerosol BrC over the South China Sea (SCS). In this study, water-soluble organic carbon (WSOC) in a round-year set of aerosol samples from a remote island in the northern SCS were characterized for optical properties. In-depth information about the sources and input pathways of water-soluble BrC was obtained using molecular markers and statistic tools. The highest WSOC concentrations, light absorption coefficients at 365 nm (Abs_{365}) and mass absorption efficiencies at 365 nm (MAE_{365}) were observed in winter when atmospheric outflow from mainland China and the northern Indo-China Peninsula prevailed. Through the year, primary emissions from biomass burning and urban secondary organic aerosols (SOA) & waste combustion, respectively, were observed to be associated with higher MAE_{365} (2.47 ± 0.40 m^2 g^{-1} and 1.97 ± 0.22 m^2 g^{-1}) and to be the main contributors to Abs_{365} ($22.0 \pm 3.6\%$ and $31.6 \pm 3.6\%$), while biogenic SOA showed little contribution. For the first time, microorganism/plankton primary emissions, mainly from the sea, was identified to be an important contributor to water-soluble BrC ($13.6 \pm 4.2\%$ of Abs_{365}, MAE_{365}: 0.98 ± 0.30 m^2 g^{-1}), especially in spring (31% of Abs_{365}). This implies that emissions from microorganism/plankton warrants careful consideration in the assessment of global aerosol light absorbance.

1. Introduction

Carbonaceous aerosols including organic carbon (OC) and black carbon (BC) are ubiquitous in the atmosphere. Light-absorbing carbonaceous aerosols play an important role in Earth's climate by impacting the radiative forcing (Bahadur et al., 2012; Chung and Seinfeld, 2002; Hansen et al., 1997). Generally, OC is considered to scatter light only and hence cool the climate (Bond et al., 2011). In contrast, BC is identified as the most effective light-absorbing carbonaceous material and thus, the third most important global warming factor, following carbon dioxide and methane (Bond et al., 2011, 2013). However, recent studies have pointed to the importance of brown carbon (BrC) which is a part of

* Corresponding author.
** Corresponding author.
E-mail addresses: gczhong@gig.ac.cn (G. Zhong), zhanggan@gig.ac.cn (G. Zhang).

https://doi.org/10.1016/j.atmosenv.2020.117484
Received 22 December 2019; Received in revised form 23 March 2020; Accepted 5 April 2020
Available online 10 April 2020

OC but also exhibits strong light absorption properties (Andreae and Gelencser, 2006). Different from BC, BrC shows a stronger wavelength dependence in ultraviolet wavelengths, suggesting substantial contributions of BrC to light absorption at shorter wavelengths (Yang et al., 2009). Notably, the strong ultraviolet light absorption by BrC may influence the formation of secondary organic aerosols (SOA) and atmospheric photochemistry by constraining the generation of ozone (O_3), hydroxyl (OH), hydroperoxyl (HO_2) and alkylperoxy (RO_2) (Jacobson, 1999; Liu et al., 2011; Mok et al., 2016).

BrC in particulate matters can be measured by optical instruments, such as particle-soot absorption photometer, aethalometer, multi-angle absorption photometer, and photo-acoustic soot spectrometer (Favez et al., 2009; Healy et al., 2015). However, it is a challenge to separate BrC from other components that could absorb or scatter light in particulate matters (Coen et al., 2010). In addition, aerosol humidity and the multiple scattering effects of filters could increase the measurement uncertainty (Coen et al., 2010). By extracting filter samples with ultrapure water or organic solvent and measuring the absorbance of extracts by spectrophotometry, some interference from other light-absorbing materials (e.g. dust) can be avoided.

Water-soluble BrC is a hot topic as it can take part in the cloud condensation nuclei (CCN) activity, radiative processes and hence influence climate forcing (Gelencser et al., 2003; Mayol-Bracero et al., 2002). Water-soluble organic carbon (WSOC) is usually used to study water-soluble BrC (Liu et al., 2013). Humic-like substance (HULIS) is a class of high molecular weight compounds isolated from WSOC operationally by solid-phase extraction (SPE). Given that HULIS is the main light-absorbing component of WSOC, it is also used to study the absorbance of water-soluble BrC (Mo et al., 2017; Park and Yu, 2016; Varga et al., 2001). Recently, the relationship between the chemistry of molecules and the optical properties of BrC has become a major research focus (Huang et al., 2018; Laskin et al., 2015). As reported, compounds bearing nitrogen-atoms, highly conjugated structures or high unsaturation degree were the potential brown carbon chromophores (Laskin et al., 2014; Mo et al., 2018).

Previous studies have reported that BrC is mainly from primary combustion emissions of biomass, biofuel and fossil fuel (Bond, 2001; Chen and Bond, 2010). In addition to primary emissions, BrC can be generated from atmospheric processes (e.g., photooxidation of aromatics, terpenes, isoprene, limonene, etc.) (Lin et al., 2014; Liu et al., 2016). It is worth noting that the sources of BrC will influence its chemical compositions and further impact light-absorbing properties. Other factors such as combustion conditions, atmospheric aging, formation pathway, and precursors may also influence BrC absorbance (Du et al., 2014; Liu et al., 2016; Saleh et al., 2014; Updyke et al., 2012).

The relationship between sources and BrC absorbance has been explored by collecting source samples, chamber experiments, and field experiments. Given that atmospheric aging and SOA formation may change aerosol light absorption (Liu et al., 2016; Srinivas and Sarin, 2014), the optical properties of aerosols obtained from source samples and chamber experiments may not accurately represent those of ambient aerosols. In field experiments, optical properties and dual-isotope carbon analysis of WSOC and HULIS were measured (Bosch et al., 2014; Kirillova et al., 2014; Liu et al., 2018; Mo et al., 2018). However, the sources of light absorption coefficient at 365 nm (Abs_{365}) and corresponding mass absorption efficiency at 365 nm (MAE_{365}) can not be quantified. Although a few studies input the raw data of Abs_{365} to a Positive Matrix Factorization (PMF) model to apportion the sources of Abs_{365} (Du et al., 2014; Hecobian et al., 2010), the relationships/pathways between BrC absorbance and its sources still require further detailed study.

Aerosols over Asia are supposed to contain considerable BrC, since major sources of BrC such as biomass burning and fossil fuel combustion are extensive in Asia (Reddy and Venkataraman, 2002; Streets et al., 2003). For instance, in 2003, the annual estimates of open-air biomass burning in Asia were about 730 Tg with China contributing 25% of this total (Streets et al., 2003). Additionally, the consumption of coal and petroleum is also huge in China (Yan et al., 2017). With high emissions from biomass burning, a high diversity of combustion types and relatively concentrated burning seasons, the Indo-China Peninsula (ICP) has been considered as a typical biomass burning region in the world (Lee et al., 2011; Lin et al., 2013a; Menzel and Prins, 1996). Located in South Asia, the northern South China Sea (SCS) is expected to receive carbonaceous aerosols from the adjacent lands (Geng et al., 2019). Meanwhile, atmospheric aging and SOA formation may occur during long-range transport, which may lead to a higher fraction of water-soluble organics and changed aerosol light absorption characteristics (Aggarwal and Kawamura, 2009; Bosch et al., 2014; Liu et al., 2016; Srinivas and Sarin, 2014). As a result, the light-absorbing properties of aerosols over the SCS are potentially influenced by water-soluble BrC or its precursors from adjacent mainland areas. Furthermore, sea surface temperature, tropical cyclones, precipitation and regional climate are likely to be influenced by changes in the light-absorbing properties of aerosols over the SCS, a marginal sea (Penner et al., 2001; Suntharalingam, 2016). Therefore, it is of importance to understand the water-soluble BrC absorbance of SCS and its sources, but data remains sparse.

A one-year aerosol sampling campaign was conducted on Xieyang Island, a small island located in the northern SCS, with the aim of characterizing the light absorption properties of water-soluble BrC in aerosols over the northern SCS and quantifying their sources. In the present study, optical properties of water-soluble BrC were investigated by the measurement of optical parameters of WSOC, viz., absorption Ångstrom exponent (AAE), MAE_{365} and Abs_{365}. The sources of WSOC were identified and quantified by PMF model and multiple molecular markers. In addition, the MAE_{365} values of WSOC from different source types and source apportionment of Abs_{365} were calculated by multiple linear regression analysis (MLRA). A Potential Source Contribution Function (PSCF) model was also applied to further define the source regions of each source type.

2. Materials and methods

2.1. Sampling

Ambient fine particulate matter ($PM_{2.5}$) samples were collected with a high volume air sampler (24 h, 1 m^3 min^{-1}) on Xieyang Island (20.908°N, 109.214°E, a small island located in the northern SCS) from 31 May 2015 to 30 May 2016. Local contamination is very limited as there are only dozens of people living on the island as fishermen. More importantly, more than 70% of the air masses arriving over Xieyang Island were from the adjacent mainland (Geng et al., 2019). Hence, Xieyang Island is a good sampling site to study the atmospheric outflow from the mainland. Details about sampling are provided elsewhere (Geng et al., 2019).

2.2. Measurements of WSOC and light absorption

An aliquot of each loaded filter was extracted with ultrapure water (20 mL, resistivity $>$ 18.2 MΩ cm) by an ultrasonicator for 30 min. The extract was then filtered through a syringe filter (25 mm $\times$ 0.22 μm, PTFE membrane, Anpel, China) to remove particles and filter chips. Following this, the carbon content of WSOC and corresponding UV–visible spectra (200–800 nm) was detected by a total organic carbon analyzer (Vario TOC cube, Elementar, Germany) and UV–visible spectrophotometer (UV-4802, Unico, China), respectively. Before the detection of carbon content, phosphoric acid (Sigma-Aldrich) was added to remove carbonates and carbon dioxide. See Supporting Information (SI) for the calculation of WSOC optical parameters, viz., AAE, MAE_{365} and Abs_{365}.

2.3. Measurements of molecular markers

The molecular markers of primary emissions measured in this study include anhydrosugars (including levoglucosan, galactosan and mannosan), vanillic acid, syringic acid, vanillin, *n*-alkanes (C_{23}–C_{35}), polycyclic aromatic hydrocarbons (PAHs, including fluoranthene (Flua), pyrene (Pyr), benzo[a]anthracene (BaA), chrysene (Chr), benzo[b]fluoranthene (BbF), benzo[k]fluoranthene (BkF), benzo[a]pyrene (BaP), dibenzo[a,h]anthracene (DahA), benzo[g,h,i]perylene (BghiP) and indeno[1,2,3-c,d]pyrene (InP)), steranes & hopanes (including ααα 20R 24R-ethylcholestane, 17α(H),21β(H)-22R-homohopane, 17α(H),21β(H)–22S-homohopane and αββ 20R 24R-ethylcholestane), terephthalic acid, sugar alcohols (including mannitol, arabitol and erythritol), oleic acid, higher molecular weight fatty acids (HFAs, C_{20}–C_{30}) and lower molecular weight fatty acids (LFAs, C_{10}–C_{18}). The methodology used to analyze these molecular markers has been provided elsewhere (Geng et al., 2019).

SOA tracers measured in this study include MGA (2-methylglyceric acid), C_5-alkene triols (including cis-2-Methyl-1,3,4-trihydroxy-1-butene, 3-Methyl-2,3,4-trihydroxy-1-butene and trans-2-Methyl-1,3,4-trihydroxy-1-butene), MTLs (including 2-methylthreitol and 2-methylerythritol), β-caryophyllinic acid, adipic acid and azelaic acid. The pretreatment of SOA tracers was same as other polar biomarkers, and details have been provided elsewhere (Geng et al., 2019). The gas chromatograph mass spectrometer (GC-MS) response factors of adipic acid and azelaic acid were determined by authentic standards. But the GC-MS response factors of MGA, MTLs and C_5-alkene triols were replaced by that of erythritol, and the response factor of β-caryophyllinic acid was replaced by that of octadecanoic acid (Li et al., 2013).

2.4. Air mass back trajectories

Five-day back trajectories were generated by Hybrid Single-particle Lagrangian Integrated Trajectory (HYSPLIT) model (http://www.arl.noaa.gov/HYSPLIT.php), with details provided elsewhere (Geng et al., 2019).

2.5. Positive Matrix Factorization (PMF) model

PMF is a receptor model that can be applied for source apportionment (Jaeckels et al., 2007). In this study, the concentrations of WSOC and multiple biomarkers were applied to the model of EPA PMF 5.0 to enable source apportionment of WSOC. Details of PMF analysis were described in SI.

2.6. Potential Source Contribution Function (PSCF) model

The PSCF model can be applied for a source region identification by dividing the potential source area into grid cells of i × j (Jain et al., 2017; Li et al., 2017; Zhang et al., 2010). In general, $PSCF_{ij}$ ranges from 0 to 1. The higher $PSCF_{ij}$ represents the higher possibility of the ijth cell being the source region. See SI for the details of PSCF principle.

2.7. Quality assurance and quality control

Three field blanks were collected to quantify and eliminate any background contamination. The mean concentration of WSOC in field blanks was 27 ± 12% of WSOC concentrations in samples, so all concentrations of WSOC in this study were corrected by the field blank values. Blanks of WSOC absorbance (330–700 nm) and SOA tracers were negligible. The recoveries of adipic acid, azelaic acid, erythritol and octadecanoic acid were 72 ± 10%, 75 ± 10%, 87 ± 5% and 105 ± 4%, respectively. There was no recovery-correction for the concentrations of SOA tracers.

3. Results and discussion

3.1. WSOC concentrations

WSOC significantly correlated with Abs_{365} ($r = 0.86$, $p < 0.01$), suggesting that BrC chromophores were important components of WSOC. WSOC averaged at 2.11 ± 1.53 μg C m^{-3} and showed the highest concentrations in February (4.88 ± 4.21 μg C m^{-3}) during winter, followed by October (3.73 ± 1.71 μg C m^{-3}) in the fall (Fig. 1). Air mass back trajectories analysis indicates that aerosols of the sampling site were mainly from South China (SC) and northern ICP in fall and winter (Fig. S1). Therefore, SC and the northern ICP appear to be the main source regions for WSOC in the northern SCS.

3.2. Light-absorbing properties of WSOC

AAE, Abs_{365} and MAE_{365} are typical optical parameters for characterizing BrC and are related to sources of BrC (Yan et al., 2014, 2017). AAE reflects the dependence of aerosol light absorption on wavelengths. MAE_{365} is generally used to describe the absorption capacity of WSOC, and is related to the chemical composition of WSOC. The chemical composition of WSOC is influenced by the sources and atmospheric reaction/aging. Abs_{365} is generally used as the surrogate of BrC absorption to avoid interference from non-organic compounds and keep consistent with previous studies. Abs_{365} is determined by emission loads and absorption capacity.

3.2.1. AAE of WSOC

Generally, BC exhibits a weak wavelength dependence, with an AAE close to unity (Bond, 2001). However, the light absorption of BrC increases sharply towards shorter wavelengths and the AAE of BrC is much higher (Yang et al., 2009). Therefore, AAE can be used to distinguish BC and BrC even though the threshold value is uncertain (Laskin et al., 2015). Throughout the year, AAE of WSOC in the present study averaged 4.83 ± 0.62, corroborating the observation that WSOC has a wavelength dependence (Roden et al., 2006). There were no distinct temporal variations of AAE values in the present study (Fig. 1), which was similar to results for samples measured in urban Xi'an (Huang et al., 2018). The mean value of AAE in the present study was lower than those measured in the South Asian outflow over the Indian Ocean (7.2 ± 0.7) (Bosch et al., 2014) and North China outflow over the Yellow Sea (6.4 ± 0.6) (Kirillova et al., 2014). Given that the absorption of molecules with a higher degree of conjugation could extend to longer wavelengths, and lead to a lower AAE (Zhang et al., 2013), molecules in aerosols of the northern SCS may, therefore, have a higher degree of conjugation than those in aerosols of the Indian Ocean and the Yellow Sea.

3.2.2. Abs_{365} of WSOC

The values of Abs_{365} averaged 3.34 ± 3.45 Mm^{-1}, which were higher than measured in remote marine aerosols in other studies (0.1–0.5 Mm^{-1} in the Indian Ocean, Maldives) (Bosch et al., 2014) but was lower than measured in large cities (10.22 ± 6.93 Mm^{-1} in Beijing and 4.48 ± 2.97 Mm^{-1} in Nanjing) (Cheng et al., 2016; Xie et al., 2020). The mean value of Abs_{365} in our study was similar to values measured over the Indo-Gangetic Plain (IGP) during summer (2.1 ± 1.4 Mm^{-1}) but much lower than those in the IGP under conditions of active biomass burning (9.7 ± 7.8 Mm^{-1}) (Rana et al., 2019).

As shown in Fig. 1, Abs_{365} showed higher values in winter (6.75 ± 6.69 Mm^{-1}) with highest values in February (12.10 ± 10.39 Mm^{-1}), followed by lower but elevated values in the fall (2.73 ± 1.46 Mm^{-1}), spring (2.70 ± 1.19 Mm^{-1}) and summer (2.07 ± 1.16 Mm^{-1}). Similar patterns of seasonal variation were also reported in urban areas of China, Korea and the United States (Du et al., 2014; Hecobian et al., 2010; Kim et al., 2016; Xie et al., 2020). In winter, air masses were mainly from SC and northern ICP, with about 20% of air masses from northern India (Fig. S1). Also, the Abs_{365} values in our study

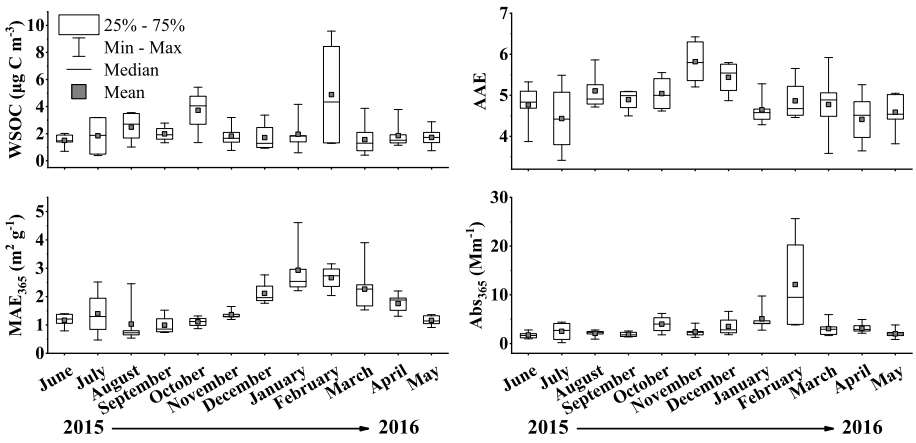

Fig. 1. Temporal variations of WSOC concentrations, AAE, MAE_{365} and Abs_{365}.

(1.82–25.63 Mm^{-1}) were similar to values reported for the IGP (2-21 Mm^{-1}) in winter (Srinivas and Sarin, 2014). Although there was no report of Abs_{365} of WSOC in $PM_{2.5}$ of SC or northern ICP, the annual average Abs_{365} of WSOC in our study was similar to that measured in PM_{10} of Guangzhou (3.57 ± 1.34 Mm^{-1}) (Liu et al., 2018). Hence, there was an enhanced land outflow of water-soluble BrC to the northern SCS in winter.

3.2.3. MAE_{365} of WSOC

The MAE_{365} values at the sampling site (1.67 ± 0.78 m^2 g^{-1}) were higher than those reported for the Indian Ocean (0.5 ± 0.2 m^2 g^{-1}) (Bosch et al., 2014) and the Yellow Sea (0.7 ± 0.2 m^2 g^{-1}) (Kirillova et al., 2014), suggesting that the chromophore activity in the aerosols of the northern SCS was relatively intense. As shown in Fig. 1, MAE_{365} showed distinct seasonal variations with the highest values in winter (2.60 ± 0.74 m^2 g^{-1}), moderate values in spring (1.71 ± 0.62 m^2 g^{-1}) but relatively lower values in summer (1.18 ± 0.64 m^2 g^{-1}) and fall (1.17 ± 0.28 m^2 g^{-1}). The temporal variations of MAE_{365} maybe because that source regions and source types of BrC varied in different seasons.

3.3. Characterization and Source Apportionment of water-soluble BrC

3.3.1. Source Apportionment of WSOC by PMF and PSCF

PMF and PSCF analysis enable the sources of WSOC to be identified. As shown in Fig. S2, factor 1 is associated with high contributions of anhydrosugars and moderate levels of vanillic acid, syringic acid, vanillin and PAHs. Anhydrosugars are typical biomarkers of biomass burning as they are exclusively from the pyrolysis of cellulose and hemicellulose (Simoneit, 2002). Vanillic acid, syringic acid and vanillin are derived from the pyrolysis of lignin, and are therefore also used to trace biomass burning aerosols (Simoneit, 2002). Furthermore, biomass burning is an important source of PAHs (Simoneit, 2002). There are also more than 20% of *n*-alkanes and HFAs in factor 1, which can also be released during biomass burning (Simoneit, 2002). Thus factor 1 indicates the primary emissions from biomass burning.

Factor 2 is characterized by high loadings of SOA tracers, such as adipic acid, β-caryophyllinic acid, MGA and azelaic acid (Fig. S2). Adipic acid is the oxidative product of anthropogenic cyclohexene which has been reported in engine exhaust and urban aerosols (Grosjean and Fung, 1984; Kawamura and Usukura, 1993). MGA is derived from isoprene photooxidation through nitrogen oxides (NO_x) pathway (Ding et al., 2016; Lin et al., 2013b). Azelaic acid and β-caryophyllinic acid are SOA tracers formed through the oxidation of O_3 with oleic acid and β-Caryophyllene, respectively (Jaoui et al., 2003, 2007; Kawamura and Gagosian, 1987). Considering that those SOA tracers are generated through NO_x/O_3 pathway and that urban aerosols have strong NO_x/O_3 production (Ding et al., 2013; Pathak et al., 2009; Wang et al., 2006), factor 2 is likely to be associated with urban SOA. Apart from SOA tracers, factor 2 also shows high/moderate loadings of molecular markers from combustion, such as terephthalic acid (originating from plastic materials combustion), PAHs (being generated from incomplete combustion of organic materials), vanillic acid and syringic acid (Kawamura and Pavuluri, 2010; Simoneit, 2002; Tobiszewski and Namieśnik, 2012). Hence factor 2 is assigned to urban SOA & waste combination, including the burning of plastics and plants.

Factor 3 is characterized by high loadings of MTLs and C_5-alkene triols which are typical tracers of isoprene SOA formed through OH/HO_2 pathways (Claeys et al., 2004; Ding et al., 2016; Paulot et al., 2009), with almost 30% contributions from MGA and azelaic acid. MGA is the oxidation product of isoprene (Lin et al., 2013b). Azelaic acid can be generated from the oxidation of oleic acid with OH/HO_2 radicals (Kawamura and Gagosian, 1987). Considering that the precursors of those SOA tracers are mainly from biogenic sources and that the OH/HO_2 pathways occur under less anthropogenic activities, factor 3 is considered to be associated with biogenic SOA. Factor 4 indicates the primary emissions from fossil fuel combustion as high loadings of steranes & hopanes and *n*-alkanes are correlated (Fig. S2). In this study, *n*-alkanes mainly originated from fossil fuel combustion (Geng et al., 2019). Steranes & hopanes are typical tracers of coal combustion and internal combustion engine emissions (Oros and Simoneit, 2000; Rogge et al., 1993; Simoneit, 2006).

Factor 5 is identified with microorganism/plankton primary emissions as it shows high contributions of sugar alcohols, followed by oleic acid and LFAs (Fig. S2). Generally, sugar alcohols are mainly derived from fungi, bacteria and marine plankton (Bauer et al., 2008; Burshtein et al., 2011; Gosselin et al., 2016). Oleic acid is from the direct emissions from the cell membranes of terrestrial plants and marine plankton (Fu et al., 2013). LFAs have been reported from microorganisms and marine plankton emissions (Kawamura et al., 2003).

Based on the source apportionment of WSOC by PMF and PSCF, 15.7% of WSOC was attributed to primary emissions from biomass burning (factor 1), mainly originating from SC and the northern ICP (Fig. 2 (a) & 3). Next, 28.3% of WSOC was attributed to urban SOA & waste combustion (factor 2), with similar source regions to factor 1. Factors 1&2 showed higher contributions to WSOC in winter (82%) and fall (52%, Fig. S3). Biogenic SOA (factor 3) contributed 22.7% of WSOC, also originating from SC and ICP and showing the highest contributions in summer (52%), followed by those in fall (37%). Primary emissions from fossil fuel combustion (factor 4) contributed 8.6% of WSOC, derived from both the mainland and SCS. There were no obvious seasonal variations in the contributions from factor 4. WSOC contributed by microorganism/plankton primary emissions (factor 5, 24.7%) was mainly derived from the SCS, followed by the ICP. Factor 5 showed the highest contributions to WSOC in spring (56%), followed by those in

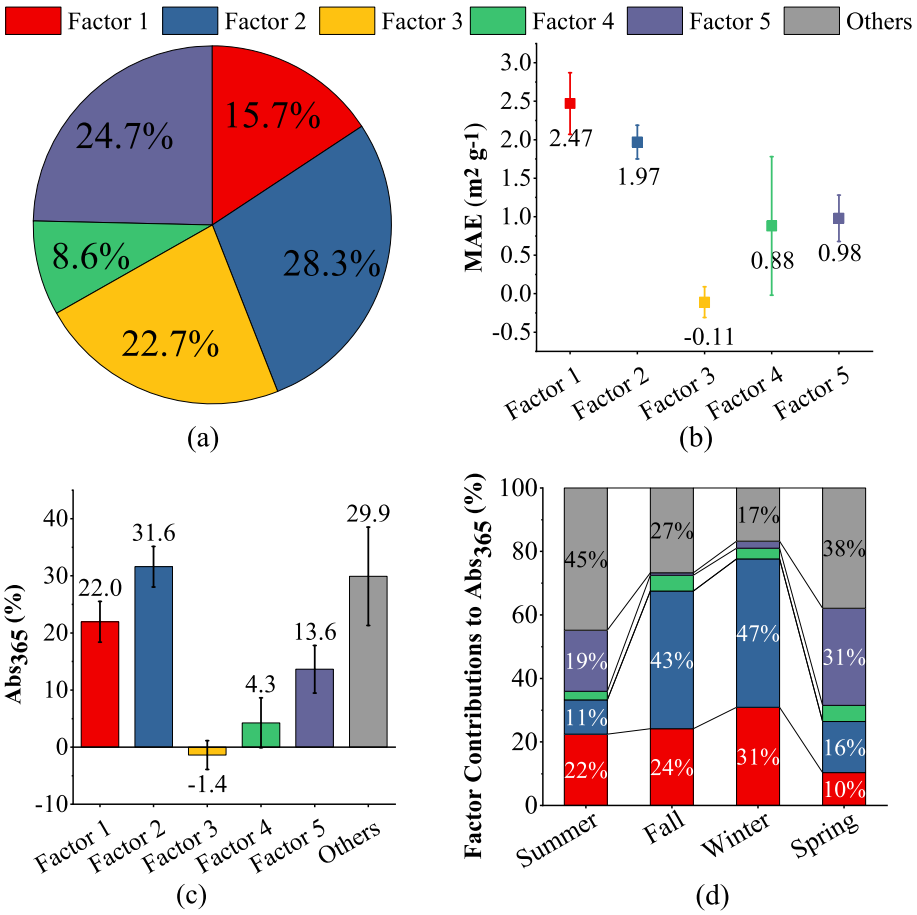

Fig. 2. (a) Contribution distribution of different sources to WSOC; (b) MAE_{365} of WSOC from different sources; (c) Contribution distribution of different sources to Abs_{365}; (d) Factor contributions to Abs_{365} in the different seasons. (Factor 1: Primary emissions from biomass burning; Factor 2: Urban SOA & waste combustion; Factor 3: Biogenic SOA; Factor 4: Primary emissions from fossil fuel combustion; Factor 5: Microorganism/plankton primary emissions.)

summer (25%). Chlorophyll-a in SCS shows a similar seasonal trend (Fig. S4), indicating that marine emissions marked by factor 5 were the major source of WSOC in the warm seasons at the study site. In summary, WSOC in aerosols over the SCS at the study site were mainly derived from the land outflow of SOA and the marine primary emissions from microorganism/plankton.

3.3.2. *Evaluation of MAE_{365} of WSOC from different sources by multiple linear regression analysis (MLRA)*

In order to evaluate the absorption capacity of WSOC from different sources, MAE_{365} of WSOC in each factor ($MAE_{365,fi}$) was calculated through the MLRA of measured Abs_{365} and modeled WSOC concentrations in different factors derived from the PMF analysis ($WSOC_{fi}$), as follows:

$$Abs_{365} = \Sigma(MAE_{365,fi} \times WSOC_{fi}) + Constant \quad (1)$$

The constant was 1.00 ± 0.29 ($p < 0.01$), suggesting that a part of Abs_{365} could not be explained by the five sources. This was reasonable as there were residuals of WSOC derived from the PMF model itself. More likely, the residuals of WSOC may cover the residuals of identified five sources and have light absorption (details were provided in SI). As shown in Fig. 2 (b), MAE_{365} explicated the highest value in primary emissions from biomass burning (2.47 ± 0.40 m^2 g^{-1}, $p < 0.01$), which was higher than measured in field experiments (1.35 ± 0.22 m^2 g^{-1} in the rural southeastern United States and 1.19 m^2 g^{-1} in Beijing) and biomass burning smoke (0.76–1.71 m^2 g^{-1}) (Du et al., 2014; Park and Yu, 2016; Washenfelder et al., 2015). The higher MAE_{365} of biomass burning emissions in the present study may be due to atmospheric aging. This inference is supported by the increased light absorption of freshly aged biomass burning aerosols in ambient and outdoor chamber experiments (Zhong and Jang, 2014). The enhanced light absorption of freshly aged biomass burning aerosols may be due to the oxidation of phenolic compounds in biomass burning emissions (Chang and Thompson, 2010; Smith et al., 2016).

The MAE_{365} in the primary emissions from fossil fuel combustion (0.88 ± 0.90 m^2 g^{-1}, $p > 0.05$) was consistent with previous studies (0.20–1.33 m^2 g^{-1}) (Du et al., 2014; Li et al., 2019). The lack of a significant regression coefficient indicated that the contribution of primary emissions from fossil fuel combustion to Abs_{365} was not significant in the aerosols of the northern SCS. If the much higher MAE_{365} of biomass burning emissions than of fossil fuel combustion emissions in the present study was generalized to other remote regions, then the influence of biomass burning on global aerosol absorption may be stronger than that of fossil fuel combustion, because the area of the planet considered remote is much larger than the area considered urban, and the contributions of biomass burning to WSOC are much higher in remote areas compared with those from fossil fuel combustion (Bosch et al., 2014; Kirillova et al., 2014).

The MAE_{365} value of microorganism/plankton primary emissions was 0.98 ± 0.30 m^2 g^{-1} ($p < 0.01$). No study has yet reported that the aerosols from microbial activities are absorbing, although an absorption contribution from phytoplankton to particles in seawater has been reported (Wang et al., 2008). In addition, microbial activities and plankton are sources of amino acids, peptide and protein (Kuznetsova et al., 2005; Milne and Zika, 1993). Generally, these compounds have higher molecular weight, nitrogen and unsaturated bonds which are the

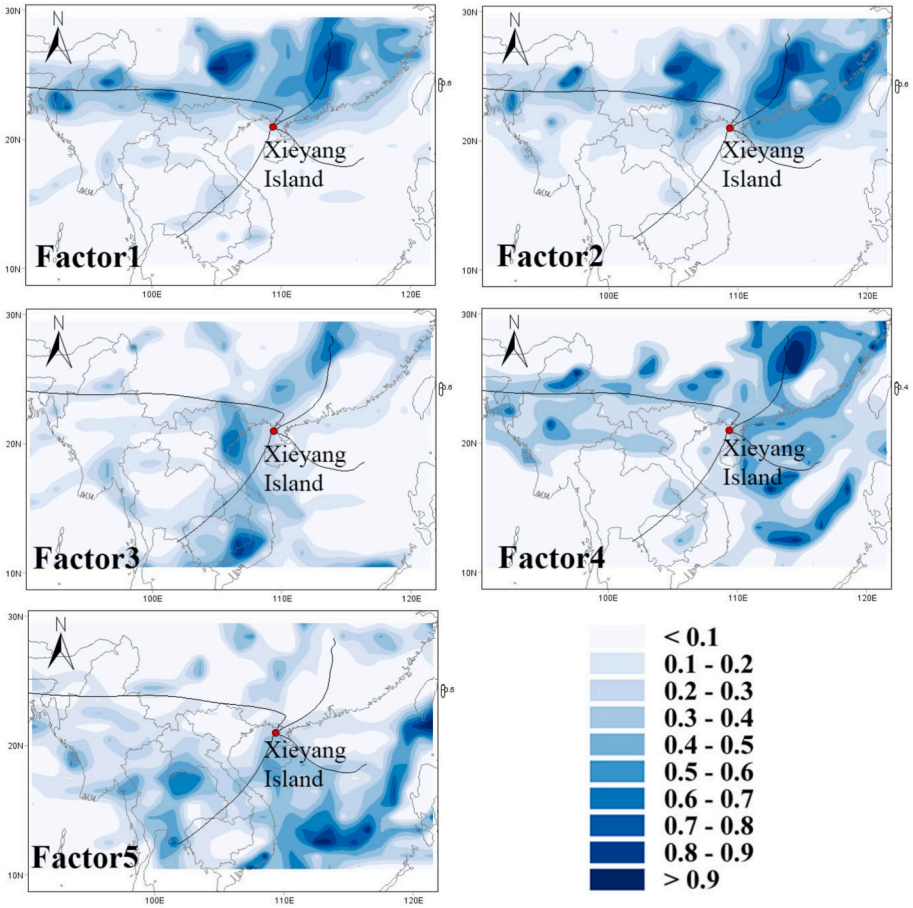

Fig. 3. Potential Source Contribution Function (PSCF) results of the five factors resolved by Positive Matrix Factorization (PMF) model. (Factor 1: Primary emissions from biomass burning; Factor 2: Urban SOA & waste combustion; Factor 3: Biogenic SOA; Factor 4: Primary emissions from fossil fuel combustion; Factor 5: Microorganism/plankton primary emissions.)

key factors influencing BrC absorption (Di Lorenzo and Young, 2016; Satish et al., 2017; Sun et al., 2007) and some amino acids have been shown to exhibit strong absorption capacity (Milne and Zika, 1993). In addition, amino acids can take part in aldol condensation and promote the formation of light absorption oligomer compounds (De Haan et al., 2010; Gao and Zhang, 2018; Haan et al., 2009; Noziere and Cordova, 2008). Significantly, these reactions are more important in marine aerosols than in non-marine aerosols (Sedehi et al., 2013). Therefore, WSOC emitted from microorganism/plankton possibly does have absorption capacity.

MAE_{365} in the factor of biogenic SOA was close to zero (-0.11 ± 0.20 m^2 g^{-1}, $p > 0.05$), which was consistent with the study carried in the rural southeastern United States (Washenfelder et al., 2015). The absence of a significant regression coefficient suggests that the contribution of biogenic SOA to Abs_{365} was negligible. The negative value of MAE_{365} may be due to the relatively large standard error. In contrast to biogenic SOA, the MAE_{365} values in the factor of urban SOA & waste combustion ranked in the second place (1.97 ± 0.22 m^2 g^{-1}, $p < 0.01$), indicating a much higher absorption capacity. This finding can be supported by previous studies those have reported that higher MAE_{365} values are observed in SOA generated from anthropogenic VOC precursors under high NO_x or O_3 conditions (Liu et al., 2016; Updyke et al., 2012). In addition, the combustion emissions of NO_x/O_3 would potentially enhance the light absorption of SOA, because that with the same biogenic/anthropogenic precursors, SOA generated through NO_x/O_3 pathways has higher MAE_{365} than SOA generated through OH/HO_2 pathways (Liu et al., 2016; Updyke et al., 2012). So, both precursors and SOA formation pathways should be considered when discussing the influence of SOA on light absorption.

3.3.3. Source Apportionment of Abs_{365}

According to the results for $MAE_{365,fi}$ and $WSOC_{fi}$, Abs_{365} of WSOC in different factors ($Abs_{365,fi}$) can be calculated as:

$$Abs_{365,fi} = MAE_{365,fi} \times WSOC_{fi} \quad (2)$$

As shown in Fig. 2 (a) & (c), although biogenic SOA contributed to 22.7% of WSOC, the contribution of biogenic SOA to Abs_{365} was close to zero ($-1.4 \pm 2.5\%$). Thus, biogenic SOA exhibited little light absorbance. In contrast, primary emissions from biomass burning was an important contributor to Abs_{365} ($22.0 \pm 3.6\%$) even though it only contributed to 15.7% of WSOC. Associated with higher MAE_{365} values and considerable contributions to WSOC, urban SOA & waste combustion was the biggest contributor to Abs_{365} ($31.6 \pm 3.6\%$). Microorganism/plankton primary emissions contributed to $13.6 \pm 4.2\%$ of Abs_{365}. The contribution of fossil fuel to Abs_{365} in the present study ($4.3 \pm 4.4\%$) was lower than that reported in Guangzhou (10%), as evaluated by dual carbon isotope composition (Liu et al., 2018). About 29.9% of Abs_{365} was from other sources. Therefore, for the identified sources, the light absorption characteristics of water-soluble BrC over the northern SCS were mainly influenced by urban SOA & waste combustion, primary emissions from biomass burning and microorganism/plankton primary emissions.

Primary emissions from biomass burning, urban SOA & waste combustion were dominated contributors to Abs_{365} in winter (78%, Fig. 2 (d)). Consequently, the highest Abs_{365} and MAE_{365} were observed in winter (Fig. 1). However, MAE_{365} showed much lower values in fall

(Fig. 1) even though primary emissions from biomass burning and urban SOA & waste combustion were still the main contributors to Abs_{365} (67%, Fig. 2 (d)). In contrast to winter, the contribution of biogenic SOC to WSOC was enhanced in the fall (Fig. S3). Hence the biogenic SOA may dilute chromophores. These findings are consistent with the results reported by an earlier laboratory study (Liu et al., 2016).

Although the contributions of microorganism/plankton primary emissions to Abs_{365} were negligible in fall and winter (less than 3%), the contributions were much higher in other seasons (Fig. 2(d)). Notably, the contribution of microorganism/plankton primary emissions to Abs_{365} was 31% in spring, which was higher than the sum of contributions (26%) from biomass burning primary emissions and urban SOA & waste combustion. Given that the contributions of anthropogenic activities to water-soluble BrC decreases in open ocean, and that microorganism/plankton primary emissions were mainly from the SCS (Fig. 3), autochthonous microorganism/plankton primary emissions could be an important contributor of water-soluble BrC in remote/global marine aerosols, especially in spring. So, emissions from microorganism/plankton may need to be included in the assessment of global aerosol light absorbance.

4. Conclusions

Based on air mass back trajectory and temporal variations in WSOC concentrations, Abs_{365} and MAE_{365}, there was an enhanced land outflow of water-soluble BrC with high light absorption capacity to the northern SCS in winter.

According to the comprehensive analysis of multiple organic molecular markers, PMF modeling and MLRA, the source types of WSOC and Abs_{365} were identified, and the MAE_{365} values of WSOC from different identified sources were calculated. With the highest MAE_{365} (2.47 ± 0.40 m^2 g^{-1}), primary emissions from biomass burning contributed to $22.0 \pm 3.6\%$ of Abs_{365} although it only comprised 15.7% of WSOC. MAE_{365} (0.88 ± 0.90 m^2 g^{-1}) and contributions of primary emissions from fossil fuel combustion to WSOC (8.6%) and Abs_{365} (4.4%) were much lower than the primary emissions from biomass burning. This implies that the influence of biomass burning on remote aerosol absorption may be stronger than that of fossil fuel combustion.

Biogenic SOA was an important contributor to WSOC (22.7%), while its' MAE_{365} and contribution to Abs_{365} was close to zero, indicating that biogenic SOA does not contribute significantly to absorbance. In contrast, the MAE_{365} of urban SOA & waste combustion was higher (1.97 ± 0.22 m^2 g^{-1}), and the contribution of urban SOA & waste combustion to WSOC (28.3%) and Abs_{365} ($31.6 \pm 3.6\%$) were considerable. Thus, the precursors and formation pathways of SOA play an important role in determining the light absorption of BrC.

Microorganism/plankton primary emissions showed moderate MAE_{365} (0.98 ± 0.30 m^2 g^{-1}) and contributions to WSOC (24.7%) and Abs_{365} ($13.6 \pm 4.2\%$). Notably, microorganism/plankton primary emissions exhibited the highest contributions to Abs_{365} in spring (31%). This implies that emissions from microorganism/plankton may need to be considered in the assessment of global aerosol light absorbance.

The results of PSCF showed that mainland was the major source region of WSOC in the northern SCS apart from microorganism/plankton primary emissions that were mainly derived from the SCS. In summary, the atmospheric outflow of primary combustion emissions and their SOA derivatives from the mainland, as well as microorganism/plankton marine emissions, were the major sources of water-soluble BrC in the northern SCS.

Declaration of competing interest

The authors declare that they have no known competing financial interests or personal relationships that could have appeared to influence the work reported in this paper.

CRediT authorship contribution statement

Xiaofei Geng: Conceptualization, Software, Validation, Formal analysis, Investigation, Writing - original draft, Writing - review & editing, Visualization. **Yangzhi Mo:** Methodology. **Jun Li:** Resources, Writing - review & editing, Funding acquisition. **Guangcai Zhong:** Writing - review & editing. **Jiao Tang:** Methodology. **Hongxing Jiang:** Methodology. **Xiang Ding:** Methodology, Writing - review & editing. **Riffat Naseem Malik:** Writing - review & editing. **Gan Zhang:** Conceptualization, Resources, Data curation, Writing - review & editing, Supervision, Project administration, Funding acquisition.

Acknowledgments

The authors thank Prof. Dr. Michael Bird for valuable comments and suggestions. The authors declare that they have neither known competing financial interests or personal relationships that could have appeared to influence the work reported in this paper. This work is funded by the National Natural Science Foundation of China (NSFC; 41430645 and 41773120), the National Key R&D Program of China (2017YFC0212000), the International Partnership Program of Chinese Academy of Sciences (132744KYSB20170002), and China Scholarship Council. The authors gratefully acknowledge the NOAA Air Resources Laboratory (ARL) for the provision of the HYSPLIT transport and dispersion model used in this publication. We acknowledge the use of imagery from MODIS. The assistance of several graduate students in our laboratories and fieldwork is kindly acknowledged. Engineers of Yankuan Tian, Jiazhuo He and Kechang Li are appreciated for maintenance of GC-MS and total organic carbon analyzer. Data sets for this research are available at ds01. Concentrations of WSOC and Optical Parameters; ds02. PMF Input Data; ds03. PMF Output; ds04. MLRA Data; ds05. PSCF Input Data.

Appendix A. Supplementary data

Supplementary data to this article can be found online at https://doi.org/10.1016/j.atmosenv.2020.117484.

References

Mayol-Bracero, O., Guyon, P., Graham, B., Roberts, G., Andreae, M., Decesari, S., Facchini, M., Fuzzi, S., Artaxo, P., 2002. Water-soluble organic compounds in biomass burning aerosols over Amazonia 2. Apportionment of the chemical composition and importance of the polyacidic fraction. J. Geophys. Res. Atmos. 107. LBA 59-51-LBA 59-15.

Aggarwal, S.G., Kawamura, K., 2009. Carbonaceous and inorganic composition in long-range transported aerosols over northern Japan: implication for aging of water-soluble organic fraction. Atmos. Environ. 43, 2532–2540.

Andreae, M.O., Gelencser, A., 2006. Black carbon or brown carbon? The nature of light-absorbing carbonaceous aerosols. Atmos. Chem. Phys. 6, 3131–3148.

Bahadur, R., Praveen, P.S., Xu, Y., Ramanathan, V., 2012. Solar absorption by elemental and brown carbon determined from spectral observations. P. Natl. Acad. Sci. USA 109, 17366–17371.

Bauer, H., Claeys, M., Vermeylen, R., Schueller, E., Weinke, G., Berger, A., Puxbaum, H., 2008. Arabitol and mannitol as tracers for the quantification of airborne fungal spores. Atmos. Environ. 42, 588–593.

Bond, T.C., 2001. Spectral dependence of visible light absorption by carbonaceous particles emitted from coal combustion. Geophys. Res. Lett. 28, 4075–4078.

Bond, T.C., Zarzycki, C., Flanner, M.G., Koch, D.M., 2011. Quantifying immediate radiative forcing by black carbon and organic matter with the Specific Forcing Pulse. Atmos. Chem. Phys. 11, 1505–1525.

Bond, T.C., Doherty, S.J., Fahey, D.W., Forster, P.M., Berntsen, T., DeAngelo, B.J., Flanner, M.G., Ghan, S., Kaercher, B., Koch, D., Kinne, S., Kondo, Y., Quinn, P.K., Sarofim, M.C., Schultz, M.G., Schulz, M., Venkataraman, C., Zhang, H., Zhang, S., Bellouin, N., Guttikunda, S.K., Hopke, P.K., Jacobson, M.Z., Kaiser, J.W., Klimont, Z., Lohmann, U., Schwarz, J.P., Shindell, D., Storelvmo, T., Warren, S.G., Zender, C.S., 2013. Bounding the role of black carbon in the climate system: a scientific assessment. J. Geophys. Res. Atmos. 118, 5380–5552.

Bosch, C., Andersson, A., Kirillova, E.N., Budhavant, K., Tiwari, S., Praveen, P.S., Russell, L.M., Beres, N.D., Ramanathan, V., Gustafsson, O., 2014. Source-diagnostic dual-isotope composition and optical properties of water-soluble organic carbon and elemental carbon in the South Asian outflow intercepted over the Indian Ocean. J. Geophys. Res. Atmos. 119, 11743–11759.

Burshtein, N., Lang-Yona, N., Rudich, Y., 2011. Ergosterol, arabitol and mannitol as tracers for biogenic aerosols in the eastern Mediterranean. Atmos. Chem. Phys. 11, 829–839.
Chang, J.L., Thompson, J.E., 2010. Characterization of colored products formed during irradiation of aqueous solutions containing H2O2 and phenolic compounds. Atmos. Environ. 44, 541–551.
Chen, Y., Bond, T.C., 2010. Light absorption by organic carbon from wood combustion. Atmos. Chem. Phys. 10, 1773–1787.
Cheng, Y., He, K.-b., Du, Z.-y., Engling, G., Liu, J.-m., Ma, Y.-l., Zheng, M., Weber, R.J., 2016. The characteristics of brown carbon aerosol during winter in Beijing. Atmos. Environ. 127, 355–364.
Chung, S.H., Seinfeld, J.H., 2002. Global distribution and climate forcing of carbonaceous aerosols. J. Geophys. Res. Atmos. 107.
Claeys, M., Graham, B., Vas, G., Wang, W., Vermeylen, R., Pashynska, V., Cafmeyer, J., Guyon, P., Andreae, M.O., Artaxo, P., Maenhaut, W., 2004. Formation of secondary organic aerosols through photooxidation of isoprene. Science 303, 1173–1176.
Coen, M.C., Weingartner, E., Apituley, A., Ceburnis, D., Fierz-Schmidhauser, R., Flentje, H., Henzing, J.S., Jennings, S.G., Moerman, M., Petzold, A., Schmid, O., Baltensperger, U., 2010. Minimizing light absorption measurement artifacts of the Aethalometer: evaluation of five correction algorithms. Atmos. Meas. Tech. 3, 457–474.
De Haan, D.O., Hawkins, L.N., Kononenko, J.A., Turley, J.J., Corrigan, A.L., Tolbert, M. A., Jimenez, J.L., 2010. Formation of nitrogen-containing oligomers by methylglyoxal and amines in simulated evaporating cloud droplets. Environ. Sci. Technol. 45, 984–991.
Di Lorenzo, R.A., Young, C.J., 2016. Size separation method for absorption characterization in brown carbon: application to an aged biomass burning sample. Geophys. Res. Lett. 43, 458–465.
Ding, A., Fu, C., Yang, X., Sun, J., Zheng, L., Xie, Y., Herrmann, E., Nie, W., Petäjä, T., Kerminen, V.-M., 2013. Ozone and fine particle in the western Yangtze River Delta: an overview of 1 yr data at the SORPES station. Atmos. Chem. Phys. 13, 5813–5830.
Ding, X., He, Q.F., Shen, R.Q., Yu, Q.Q., Zhang, Y.Q., Xin, J.Y., Wen, T.X., Wang, X.M., 2016. Spatial and seasonal variations of isoprene secondary organic aerosol in China: significant impact of biomass burning during winter. Sci. Rep. 6, 20411.
Du, Z., He, K., Cheng, Y., Duan, F., Ma, Y., Liu, J., Zhang, X., Zheng, M., Weber, R., 2014. A yearlong study of water-soluble organic carbon in Beijing II: light absorption properties. Atmos. Environ. 89, 235–241.
Favez, O., Cachier, H., Sciare, J., Sarda-Esteve, R., Martinon, L., 2009. Evidence for a significant contribution of wood burning aerosols to PM2.5 during the winter season in Paris, France. Atmos. Environ. 43, 3640–3644.
Fu, P.Q., Kawamura, K., Chen, J., Charrière, B., Sempéré, R., 2013. Organic molecular composition of marine aerosols over the Arctic Ocean in summer: contributions of primary emission and secondary aerosol formation. Biogeosciences 10, 653–667.
Gao, Y., Zhang, Y., 2018. Formation and photochemical investigation of brown carbon by hydroxyacetone reactions with glycine and ammonium sulfate. RSC Adv. 8, 20719–20725.
Gelencser, A., Hoffer, A., Kiss, G., Tombacz, E., Kurdi, R., Bencze, L., 2003. In-situ formation of light-absorbing organic matter in cloud water. J. Atmos. Chem. 45, 25–33.
Geng, X., Zhong, G., Li, J., Cheng, Z., Mo, Y., Mao, S., Su, T., Jiang, H., Ni, K., Zhang, G., 2019. Molecular marker study of aerosols in the northern South China sea: impact of atmospheric outflow from the Indo-China Peninsula and South China. Atmos. Environ. 206, 225–236.
Gosselin, M.I., Rathnayake, C.M., Crawford, I., Pöhlker, C., Fröhlich-Nowoisky, J., Schmer, B., Després, V.R., Engling, G., Gallagher, M., Stone, E., Pöschl, U., Huffman, J.A., 2016. Fluorescent bioaerosol particle, molecular tracer, and fungal spore concentrations during dry and rainy periods in a semi-arid forest. Atmos. Chem. Phys. 16, 15165–15184.
Grosjean, D., Fung, K., 1984. Hydrocarbons and carbonyls in Los Angeles air. J. Air Pollut. Contr. Assoc. 34, 537–543.
Haan, D.O.D., Corrigan, A.L., Smith, K.W., Stroik, D.R., Turley, J.J., Lee, F.E., Tolbert, M. A., Jimenez, J.L., Cordova, K.E., Ferrell, G.R., 2009. Secondary organic aerosol-forming reactions of glyoxal with amino acids. Environ. Sci. Technol. 43, 2818–2824.
Hansen, J., Sato, M., Ruedy, R., 1997. Radiative forcing and climate response. J. Geophys. Res. Atmos. 102, 6831–6864.
Healy, R.M., Wang, J.M., Jeong, C.H., Lee, A.K.Y., Willis, M.D., Jaroudi, E., Zimmerman, N., Hilker, N., Murphy, M., Eckhardt, S., Stohl, A., Abbatt, J.P.D., Wenger, J.C., Evans, G.J., 2015. Light-absorbing properties of ambient black carbon and brown carbon from fossil fuel and biomass burning sources. J. Geophys. Res. Atmos. 120, 6619–6633.
Hecobian, A., Zhang, X., Zheng, M., Frank, N., Edgerton, E.S., Weber, R.J., 2010. Water-Soluble Organic Aerosol material and the light-absorption characteristics of aqueous extracts measured over the Southeastern United States. Atmos. Chem. Phys. 10, 5965–5977.
Huang, R.-J., Yang, L., Cao, J., Chen, Y., Chen, Q., Li, Y., Duan, J., Zhu, C., Dai, W., Wang, K., Lin, C., Ni, H., Corbin, J.C., Wu, Y., Zhang, R., Tie, X., Hoffmann, T., O'Dowd, C., Dusek, U., 2018. Brown carbon aerosol in urban Xi'an, Northwest China: the composition and light absorption properties. Environ. Sci. Technol. 52, 6825–6833.
Jacobson, M.Z., 1999. Isolating nitrated and aromatic aerosols and nitrated aromatic gases as sources of ultraviolet light absorption. J. Geophys. Res. Atmos. 104, 3527–3542.
Jaeckels, J.M., Bae, M.S., Schauer, J.J., 2007. Positive matrix factorization (PMF) analysis of molecular marker measurements to quantify the sources of organic aerosols. Environ. Sci. Technol. 41, 5763–5769.
Jain, S., Sharma, S.K., Choudhary, N., Masiwal, R., Saxena, M., Sharma, A., Mandal, T.K., Gupta, A., Gupta, N.C., Sharma, C., 2017. Chemical characteristics and source apportionment of PM2.5 using PCA/APCS, UNMIX, and PMF at an urban site of Delhi, India. Environ. Sci. Pollut. Res. 24, 14637–14656.
Jaoui, M., Leungsakul, S., Kamens, R.M., 2003. Gas and particle products distribution from the reaction of β-caryophyllene with ozone. J. Atmos. Chem. 45, 261–287.
Jaoui, M., Lewandowski, M., Kleindienst, T.E., Offenberg, J.H., Edney, E.O., 2007. β-caryophyllinic acid: an atmospheric tracer forβ-caryophyllene secondary organic aerosol. Geophys. Res. Lett. 34.
Kawamura, K., Gagosian, R.B., 1987. Implications of omega-oxocarboxylic acids in the remote marine atmosphere for photooxidation of unsaturated fatty-acids. Nature 325, 330–332.
Kawamura, K., Pavuluri, C.M., 2010. New Directions: need for better understanding of plastic waste burning as inferred from high abundance of terephthalic acid in South Asian aerosols. Atmos. Environ. 44, 5320–5321.
Kawamura, K., Usukura, K., 1993. Distributions of low molecular weight dicarboxylic acids in the North Pacific aerosol samples. J. Oceanogr. 49, 271–283.
Kawamura, K., Ishimura, Y., Yamazaki, K., 2003. Four years' observations of terrestrial lipid class compounds in marine aerosols from the western North Pacific. Global Biogeochem. Cycles 17, 3-1-3-19.
Kim, H., Kim, J.Y., Jin, H.C., Lee, J.Y., Lee, S.P., 2016. Seasonal variations in the light-absorbing properties of water-soluble and insoluble organic aerosols in Seoul, Korea. Atmos. Environ. 129, 234–242.
Kirillova, E.N., Andersson, A., Han, J., Lee, M., Gustafsson, O., 2014. Sources and light absorption of water-soluble organic carbon aerosols in the outflow from northern China. Atmos. Chem. Phys. 14, 1413–1422.
Kuznetsova, M., Lee, C., Aller, J., 2005. Characterization of the proteinaceous matter in marine aerosols. Mar. Chem. 96, 359–377.
Laskin, J., Laskin, A., Nizkorodov, S.A., Roach, P., Eckert, P., Gilles, M.K., Wang, B., Lee, H.J., Hu, Q., 2014. Molecular selectivity of Brown carbon chromophores. Environ. Sci. Technol. 48, 12047–12055.
Laskin, A., Laskin, J., Nizkorodov, S.A., 2015. Chemistry of atmospheric Brown carbon. Chem. Rev. 115, 4335–4382.
Lee, C.-T., Chuang, M.-T., Lin, N.-H., Wang, J.-L., Sheu, G.-R., Chang, S.-C., Wang, S.-H., Huang, H., Chen, H.-W., Liu, Y.-L., Weng, G.-H., Lai, H.-Y., Hsu, S.-P., 2011. The enhancement of PM2.5 mass and water-soluble ions of biosmoke transported from Southeast Asia over the Mountain Lulin site in Taiwan. Atmos. Environ. 45, 5784–5794.
Li, J.J., Wang, G.H., Cao, J.J., Wang, X.M., Zhang, R.J., 2013. Observation of biogenic secondary organic aerosols in the atmosphere of a mountain site in central China: temperature and relative humidity effects. Atmos. Chem. Phys. 13, 11535–11549.
Li, D., Liu, J., Zhang, J., Gui, H., Du, P., Yu, T., Wang, J., Lu, Y., Liu, W., Cheng, Y., 2017. Identification of long-range transport pathways and potential sources of PM2.5 and PM10 in Beijing from 2014 to 2015. J. Environ. Sci. (China) 56, 214–229.
Li, M., Fan, X., Zhu, M., Zou, C., Song, J., Wei, S., Jia, W., Peng, P., 2019. Abundance and light absorption properties of Brown carbon emitted from residential coal combustion in China. Environ. Sci. Technol. 53, 595–603.
Lin, N.-H., Tsay, S.-C., Maring, H.B., Yen, M.-C., Sheu, G.-R., Wang, S.-H., Chi, K.H., Chuang, M.-T., Ou-Yang, C.-F., Fu, J.S., Reid, J.S., Lee, C.-T., Wang, L.-C., Wang, J.-L., Hsu, C.N., Sayer, A.M., Holben, B.N., Chu, Y.-C., Nguyen, X.A., Sopajaree, K., Chen, S.-J., Cheng, M.-T., Tsuang, B.-J., Tsai, C.-J., Peng, C.-M., Schnell, R.C., Conway, T., Chang, C.-T., Lin, K.-S., Tsai, Y.I., Lee, W.-J., Chang, S.-C., Liu, J.-J., Chiang, W.-L., Huang, S.-J., Lin, T.-H., Liu, G.-R., 2013a. An overview of regional experiments on biomass burning aerosols and related pollutants in Southeast Asia: from BASE-ASIA and the Dongsha Experiment to 7-SEAS. Atmos. Environ. 78, 1–19.
Lin, Y.-H., Zhang, H., Pye, H.O.T., Zhang, Z., Marth, W.J., Park, S., Arashiro, M., Cui, T., Budisulistiorini, H., Sexton, K.G., Vizuete, W., Xie, Y., Luecken, D.J., Piletic, I.R., Edney, E.O., Bartolotti, L.J., Gold, A., Surratt, J.D., 2013b. Epoxide as a precursor to secondary organic aerosol formation from isoprene photooxidation in the presence of nitrogen oxides. P. Natl. Acad. Sci. USA 110, 6718–6723.
Lin, Y.H., Budisulistiorini, S.H., Chu, K., Siejack, R.A., Zhang, H., Riva, M., Zhang, Z., Gold, A., Kautzman, K.E., Surratt, J.D., 2014. Light-absorbing oligomer formation in secondary organic aerosol from reactive uptake of isoprene epoxydiols. Environ. Sci. Technol. 48, 12012–12021.
Liu, S., Day, D.A., Shields, J.E., Russell, L.M., 2011. Ozone-driven daytime formation of secondary organic aerosol containing carboxylic acid groups and alkane groups. Atmos. Chem. Phys. 11, 8321–8341.
Liu, J., Bergin, M., Guo, H., King, L., Kotra, N., Edgerton, E., Weber, R.J., 2013. Size-resolved measurements of brown carbon in water and methanol extracts and estimates of their contribution to ambient fine-particle light absorption. Atmos. Chem. Phys. 13, 12389–12404.
Liu, J., Lin, P., Laskin, A., Laskin, J., Kathmann, S.M., Wise, M., Caylor, R., Imholt, F., Selimovic, V., Shilling, J.E., 2016. Optical properties and aging of light-absorbing secondary organic aerosol. Atmos. Chem. Phys. 16, 12815–12827.
Liu, J., Mo, Y., Ding, P., Li, J., Shen, C., Zhang, G., 2018. Dual carbon isotopes ((14)C and (13)C) and optical properties of WSOC and HULIS-C during winter in Guangzhou, China. Sci. Total Environ. 633, 1571–1578.
Menzel, W.P., Prins, E.M., 1996. Monitoring biomass burning with the new generation of geostationary satellites. In: Levine, J.S. (Ed.), Biomass Burning and Global Change. MIT Press, Cambridge, pp. 56–64.
Milne, P.J., Zika, R.G., 1993. Amino acid nitrogen in atmospheric aerosols: occurrence, sources and photochemical modification. J. Atmos. Chem. 16, 361–398.
Mo, Y., Li, J., Liu, J., Zhong, G., Cheng, Z., Tian, C., Chen, Y., Zhang, G., 2017. The influence of solvent and pH on determination of the light absorption properties of water-soluble brown carbon. Atmos. Environ. 161, 90–98.

Mo, Y., Li, J., Jiang, B., Su, T., Geng, X., Liu, J., Jiang, H., Shen, C., Ding, P., Zhong, G., Cheng, Z., Liao, Y., Tian, C., Chen, Y., Zhang, G., 2018. Sources, compositions, and optical properties of humic-like substances in Beijing during the 2014 APEC summit: results from dual carbon isotope and Fourier-transform ion cyclotron resonance mass spectrometry analyses. Environ. Pollut. 239, 322–331.
Mok, J., Krotkov, N.A., Arola, A., Torres, O., Jethva, H., Andrade, M., Labow, G., Eck, T. F., Li, Z., Dickerson, R.R., 2016. Impacts of brown carbon from biomass burning on surface UV and ozone photochemistry in the Amazon Basin. Sci. Rep. 6, 36940.
Noziere, B., Cordova, A., 2008. A kinetic and mechanistic study of the amino acid catalyzed aldol condensation of acetaldehyde in aqueous and salt solutions. J. Phys. Chem. 112, 2827–2837.
Oros, D.R., Simoneit, B.R.T., 2000. Identification and emission rates of molecular tracers in coal smoke particulate matter. Fuel 79, 515–536.
Park, S.S., Yu, J., 2016. Chemical and light absorption properties of humic-like substances from biomass burning emissions under controlled combustion experiments. Atmos. Environ. 136, 114–122.
Pathak, R.K., Wu, W.S., Wang, T., 2009. Summertime PM 2.5 ionic species in four major cities of China: nitrate formation in an ammonia-deficient atmosphere. Atmos. Chem. Phys. 9, 1711–1722.
Paulot, F., Crounse, J.D., Kjaergaard, H.G., Kuerten, A., St Clair, J.M., Seinfeld, J.H., Wennberg, P.O., 2009. Unexpected epoxide formation in the gas-phase photooxidation of isoprene. Science 325, 730–733.
Penner, J.E., Hegg, D., Leaitch, R., 2001. Unraveling the role of aerosols in climate change. Environ. Sci. Technol. 35, 332A–340A.
Rana, A., Dey, S., Sarkar, S., 2019. Optical properties of atmospheric brown carbon (BrC) for photochemical and biomass burning-dominated aerosol regimes in India. In: AGU Fall Meeting 2019. AGU.
Reddy, M.S., Venkataraman, C., 2002. Inventory of aerosol and sulphur dioxide emissions from India: I - fossil fuel combustion. Atmos. Environ. 36, 677–697.
Roden, C.A., Bond, T.C., Conway, S., Benjamin, A., Pinel, O., 2006. Emission factors and real-time optical properties of particles emitted from traditional wood burning cookstoves. Environ. Sci. Technol. 40, 6750–6757.
Rogge, W.F., Hildemann, L.M., Mazurek, M.A., Cass, G.R., Simoneit, B.R.T., 1993. Sources of fine organic aerosol. 2. Noncatalyst and catalyst-equipped automobiles and heavy-duty diesel trucks. Environ. Sci. Technol. 27, 636–651.
Saleh, R., Robinson, E.S., Tkacik, D.S., Ahern, A.T., Liu, S., Aiken, A.C., Sullivan, R.C., Presto, A.A., Dubey, M.K., Yokelson, R.J., Donahue, N.M., Robinson, A.L., 2014. Brownness of organics in aerosols from biomass burning linked to their black carbon content. Nat. Geosci. 7, 647–650.
Satish, R., Shamjad, P., Thamban, N., Tripathi, S., Rastogi, N., 2017. Temporal characteristics of Brown carbon over the central Indo-Gangetic Plain. Environ. Sci. Technol. 51, 6765–6772.
Sedehi, N., Takano, H., Blasic, V.A., Sullivan, K.A., De Haan, D.O., 2013. Temperature- and pH-dependent aqueous-phase kinetics of the reactions of glyoxal and methylglyoxal with atmospheric amines and ammonium sulfate. Atmos. Environ. 77, 656–663.
Simoneit, B.R.T., 2002. Biomass burning — a review of organic tracers for smoke from incomplete combustion. Appl. Geochem. 129–162.
Simoneit, B.R.T., 2006. Application of molecular marker analysis to vehicular exhaust for source reconciliations. Int. J. Environ. Anal. Chem. 22, 203–232.
Smith, J.D., Kinney, H., Anastasio, C., 2016. Phenolic carbonyls undergo rapid aqueous photodegradation to form low-volatility, light-absorbing products. Atmos. Environ. 126, 36–44.
Srinivas, B., Sarin, M.M., 2014. Brown carbon in atmospheric outflow from the Indo-Gangetic Plain: mass absorption efficiency and temporal variability. Atmos. Environ. 89, 835–843.
Streets, D.G., Yarber, K.F., Woo, J.H., Carmichael, G.R., 2003. Biomass burning in Asia: annual and seasonal estimates and atmospheric emissions. Global Biogeochem. Cycles 17, 1099.
Sun, H., Biedermann, L., Bond, T.C., 2007. Color of brown carbon: a model for ultraviolet and visible light absorption by organic carbon aerosol. Geophys. Res. Lett. 34.
Suntharalingam, P., 2016. SOLAS 2015-2025 Science Plan and Organisation: Linking Ocean-Atmosphere Interactions with Climate and People. SOLAS International Project Office.
Tobiszewski, M., Namieśnik, J., 2012. PAH diagnostic ratios for the identification of pollution emission sources. Environ. Pollut. 162, 110–119.
Updyke, K.M., Nguyen, T.B., Nizkorodov, S.A., 2012. Formation of brown carbon via reactions of ammonia with secondary organic aerosols from biogenic and anthropogenic precursors. Atmos. Environ. 63, 22–31.
Varga, B., Kiss, G., Ganszky, I., Gelencser, A., Krivacsy, Z., 2001. Isolation of water-soluble organic matter from atmospheric aerosol. Talanta 55, 561–572.
Wang, T., Ding, A., Gao, J., Wu, W.S., 2006. Strong ozone production in urban plumes from Beijing, China. Geophys. Res. Lett. 33.
Wang, G., Cao, W., Yang, D., Zhao, J., 2008. Partitioning particulate absorption coefficient into contributions of phytoplankton and nonalgal particles: a case study in the northern South China Sea. Estuar. Coast Shelf Sci. 78, 513–520.
Washenfelder, R.A., Attwood, A.R., Brock, C.A., Guo, H., Xu, L., Weber, R.J., Ng, N.L., Allen, H.M., Ayres, B.R., Baumann, K., Cohen, R.C., Draper, D.C., Duffey, K.C., Edgerton, E., Fry, J.L., Hu, W.W., Jimenez, J.L., Palm, B.B., Romer, P., Stone, E.A., Wooldridge, P.J., Brown, S.S., 2015. Biomass burning dominates brown carbon absorption in the rural southeastern United States. Geophys. Res. Lett. 42, 653–664.
Xie, X., Chen, Y., Nie, D., Liu, Y., Liu, Y., Lei, R., Zhao, X., Li, H., Ge, X., 2020. Light-absorbing and fluorescent properties of atmospheric brown carbon: a case study in Nanjing, China. Chemosphere 126350.
Yan, C.-Q., Zheng, M., Zhang, Y.-H., 2014. Research progress and direction of atmospheric brown carbon. Huanjing Kexue 35, 4404–4414.
Yan, C., Zheng, M., Bosch, C., Andersson, A., Desyaterik, Y., Sullivan, A.P., Collett, J.L., Zhao, B., Wang, S., He, K., Gustafsson, O., 2017. Important fossil source contribution to brown carbon in Beijing during winter. Sci. Rep. 7.
Yang, M., Howell, S.G., Zhuang, J., Huebert, B.J., 2009. Attribution of aerosol light absorption to black carbon, brown carbon, and dust in China - interpretations of atmospheric measurements during EAST-AIRE. Atmos. Chem. Phys. 9, 2035–2050.
Zhang, G., Li, J., Li, X.D., Xu, Y., Guo, L.L., Tang, J.H., Lee, C.S.L., Liu, X.A., Chen, Y.J., 2010. Impact of anthropogenic emissions and open biomass burning on regional carbonaceous aerosols in South China. Environ. Pollut. 158, 3392–3400.
Zhang, X., Lin, Y.H., Surratt, J.D., Weber, R.J., 2013. Sources, composition and absorption Angstrom exponent of light-absorbing organic components in aerosol extracts from the Los Angeles Basin. Environ. Sci. Technol. 47, 3685–3693.
Zhong, M., Jang, M., 2014. Dynamic light absorption of biomass-burning organic carbon photochemically aged under natural sunlight. Atmos. Chem. Phys. 14, 1517–1525.